Biomedicine & Pharmacotherapy 157 (2023) 114012

Contents lists available at ScienceDirect

Biomedicine & Pharmacotherapy

journal homepage: www.elsevier.com/locate/biopha

Withaferin A-silyl ether analogs as potential anti-kinetoplastid agents targeting the programmed cell death

San Nicolás-Hernández Desirée [a,b,c,1], J. Bethencourt-Estrella Carlos [a,b,c], López-Arencibia Atteneri [a,b,c,d], Hernández-Álvarez Eduardo [e], Sifaoui Ines [a,b,c], L. Bazzocchi Isabel [e], Lorenzo-Morales Jacob [a,b,c,d], A. Jimenez Ignacio [e,*], E. Piñero José [a,b,c,d,**]

[a] Instituto Universitario de Enfermedades Tropicales y Salud Pública de Canarias, Universidad de La Laguna, Avda. Astrofísico Fco. Sanchez, S/N, 38203 La Laguna, Tenerife, Canary Islands, Spain
[b] Departamento de Obstetricia y Ginecología, Pediatría, Medicina Preventiva y Salud Pública, Toxicología, Medicina Legal y Forense y Parasitología, Universidad de La Laguna, 38200 La Laguna, Tenerife, Spain
[c] Red de Investigación Cooperativa en Enfermedades Tropicales (RICET), Inst. de Salud Carlos III, Madrid, Spain
[d] CIBER de Enfermedades Infecciosas (CIBERINFEC), Inst. de Salud Carlos III, Madrid, Spain
[e] Instituto Universitario de Bio-Orgánica Antonio González, Departamento de Química Orgánica, Universidad de La Laguna, Avenida Astrofísico Francisco Sánchez 2, 38206 La Laguna, Tenerife, Canary Islands, Spain

ARTICLE INFO

Keywords:
Leishmaniasis
Chagas disease
Withaferin A
Apoptosis
Autophagy

ABSTRACT

Current therapies of leishmaniasis and Chagas disease, two of the most widespread neglected tropical diseases, have limited efficacy and toxic side effects. In this regard, natural products play an important role in overcoming the current need for new antiparasitic agents. The present study reports the leishmanicidal and trypanocidal activities of twenty-four known silyl-ether derivatives of withaferin A. Eleven compounds from this series (**4**, **7**, **8**, **10**, **12**, **15**, **17**, **18**, **20**, **22** and **25**) showed a potent dose-dependent inhibitory effect on the proliferation of *Leishmania amazonensis* promastigotes and *Trypanosoma cruzi* epimastigotes respectively, even higher than the references drugs, miltefosine and benznidazole. Among them, the most promising compound, derivative **10**, exhibited approximately 34-fold higher leishmanicidal activity and 49-fold higher trypanocidal activity compared to the reference drugs, as well as lower cytotoxicity. Moreover, compounds **4**, **7**, **10**, **12** and **15** were more active than the reference drugs against the amastigote forms of *L. amazonensis*, presenting a high selectivity index. Assays performed to study the ATP levels, mitochondrial membrane potential, plasma membrane permeability, chromatin condensation, reactive oxygen species and autophagy indicated that these withaferin A-silyl analogs appear to induce events characteristic of apoptosis-like and also autophagy leading to programmed cell death. These findings support the therapeutic potential of withaferin A-related steroids as anti-*Leishmania* and *Trypanosoma* agents.

1. Introduction

Leishmaniasis and Chagas disease are neglected tropical diseases caused by the parasitic protozoa: *Leishmania* spp. and *Trypanosoma cruzi*, respectively. These diseases mostly affect populations in tropical and subtropical rural areas with precarious sanitary conditions. However, due to climate change and migratory movements, among other factors, the number of cases of both diseases has increased worldwide, even becoming endemic in some European countries, as is the case of leishmaniasis [1–4].

Abbreviations: WA, withaferin A; DMSO, dimethyl sulfoxide; PI, propidium iodide; PCD, programmed cell death; ROS, reactive oxygen species; MCD, monodansylcadaverine.

* Corresponding author.
** Correspondence to: Avda. Astrofísico Fco. Sanchez, S/N, 38203 La Laguna, Tenerife, Canary Islands, Spain.
E-mail addresses: dsannico@ull.edu.es (S.N.-H. Desirée), cbethene@ull.edu.es (J. Bethencourt-Estrella Carlos), atlopez@ull.edu.es (L.-A. Atteneri), alu0100947311@ull.edu.es (H.-Á. Eduardo), isifaoui@ull.edu.es (S. Ines), ilopez@ull.edu.es (L. Bazzocchi Isabel), jmlorenz@ull.edu.es (L.-M. Jacob), ignadiaz@ull.edu.es (A. Jimenez Ignacio), jpinero@ull.edu.es (E.P. José).
[1] ORCID: 0000-0002-6622-1928

https://doi.org/10.1016/j.biopha.2022.114012
Received 3 October 2022; Received in revised form 10 November 2022; Accepted 11 November 2022
Available online 16 November 2022

There are more than 20 species of *Leishmania* spp. which are able to infect humans through the bite of female sandflies. This parasite has two life forms in its biological cycle: promastigotes, which are present in the intestine of the vector, and amastigotes, which is an intracellular form present inside the cells of the host. There are different pathologies of leishmaniasis in patients. Some infected persons may have a silent infection while others may manifest different types of clinical manifestations. According to this, three types of leishmaniasis are described: cutaneous, mucocutaneous and visceral leishmaniasis. Cutaneous and mucocutaneous leishmaniasis are mild forms of the disease (characterized by skin lesions and damage in the mucous membranes of the nose, mouth and throat, respectively). Visceral leishmaniasis is the most lethal and dangerous of all, as it affects vital organs such as liver, spleen or bone marrow. It is estimated that this globally distributed disease causes approximately 700.000–1.2 million new cases of cutaneous leishmaniasis per year. On the other hand, the number of new cases per year of visceral leishmaniasis is approximately less than 400.000 [5,6].

Chagas disease is caused by the parasite *Trypanosoma cruzi* and is also known as American trypanosomiasis because it occurs mainly in rural areas of South America, the place on the planet where the triatomine bug is found. Infection occurs through contact with triatomine's feces. In addition, there are other forms of transmission, such as oral transmission (by ingesting food or drinks contaminated with the vector's feces), congenital transmission, organ transplants, blood transfusions or laboratory accidents. These other forms of transmission, together with population movements and emigration, have changed the geographical distribution of the disease, which in the recent decades has spread to countries all over the world. Therefore, many infected patients may remain in an asymptomatic phase of the disease throughout their lives. In other cases, 20–30% of them will end up with a chronic phase of the disease. In this phase, the parasites infect organs such as the heart and stomach, which can lead to sudden death from cardiac arrhythmia or heart failure. Currently, *ca.* 6–7 million people are infected worldwide, mainly in Latin America [3,7,8].

Available treatments present multiple limitations such as high toxicity, high cost, prolonged treatment and the development of resistant strains [9]. In view of this situation and without the possibility of vaccination, the search for new active compounds with leishmanicidal and trypanocidal activity with low toxicity for patients is urgent. In this context, traditional knowledge about medicinal plants and their properties and therapeutic uses is a fundamental tool in the search for new active compounds from natural resources and the development of new drug sources. For instance, in a previous study by López-Arencibia et al. [10], compounds with promising leishmanicidal and trypanocidal activity such as withaferin A, were isolated from the medicinal plant *Withania aristata* (Solanaceae). This plant is known for its antispasmodic and healing properties, and is also used to combat rheumatism, otitis, insomnia, urinary pathologies, constipation and rheumatism [11]. Withaferin A isolated from this plant is a natural steroidal lactone that, in addition to its promising antiparasitic activity, has demonstrated potent antitumor activity against ovarian cancer in previous studies [12,13]. Consequently, withaferin A can be considered a novel and potential anti-kinetoplastid agent.

Despite current studies suggesting that WA is a promising leishmanicidal and trypanocidal agent, the development of an antiparasitic drug has not yet been carried out. The main challenge is to obtain compounds with anti-kinetoplastid activity and low toxicity. In addition, it is important to keep in mind that these drug candidates must also interact with the patient's organism and therefore it is essential that they have a positive ADME profile (theoretical prediction of the pharmacokinetic properties of a compound: absorption, distribution, metabolism, excretion and toxicity in the organism). Many drug candidates, despite being active and not toxic, have shown a negative ADME profile, which has been identified as a major cause of failure of candidate molecules in drug development [12]. As Franz et al. explain in detail, the incorporation of silicon and the synthesis of small organosilicon molecules offer multiple medicinal applications. Differences in the chemical properties of silicon-containing molecules have resulted in better and more interesting medicinal applications compared to traditional carbon-based functional groups. These differences offer the possibility of specific interactions between an organosilicon molecule and a biological macromolecule. The various steric and substitution patterns available for organosilicon compounds offer opportunities to design and control the stability, solubility and pharmacokinetic properties of these compounds. Moreover, the strategic incorporation of silyl group into the scaffolds of drug candidate molecules (such as WA) is a method to optimize biological activity and reduce toxicity with the aim of increasing the therapeutic potential of a compound. In addition, the incorporation of silyl groups is a general strategy to increase size and lipophilicity for drug design. This may translate into an increased likelihood of obtaining a positive ADME profile of the drug candidate of interest [12,14].

In order to achieve compounds with low toxicity and no side effects in patients, it is important to elucidate how the compounds induce cell death in parasites to avoid inflammatory processes. There is currently some controversy about the types of cell death in protozoa. These organisms possess different molecular components to eukaryotes, lacking some key proteins and genes for the development of programmed cell death processes, such as some caspases involved in apoptosis, among others. It is necessary to investigate these cell death mechanisms as there could be some proteins or genes analogous to those known in eukaryotic organisms, which could be specific to protozoa. Some authors such as Proto et al. [15] propose that cell death in protozoa can be caused by only two types of cell death: necrosis (usually associated with inflammatory processes) or incidental death. On the other hand, recent studies have shown that some compounds are responsible for initiating a cascade of events characteristic of apoptosis-like in unicellular organisms such as kinetoplastids. For instance, Silva-Silva et al. reported that carajurin (the main constituent of *Arrabidaea chica*) caused ultrastructural changes, decreased mitochondrial membrane potential and increased ROS production in *L. amazonensis*. Thus, they demonstrated that this compound induced cell death by late apoptosis-like in the parasite [16]. Chiboub et al. isolated three compounds from the brown seaweed *Dictyota spiralis* and reported that the three isolated diterpenes inhibited *L.amazonensis* and *T. cruzi* by inducing an apoptosis-like cell death, as the parasites showed chromatin condensation, decrease of ATP levels and mitochondrial membrane potential, increase ROS production, among other physiological changes [17]. These observations represent the opening of a new line of research in the search for targets responsible for apoptosis-like in parasites, thus becoming possible therapeutic targets. In both parasites, some characteristic signs of programmed cell death have been observed, such as cell shrinkage, nuclear chromatin condensation, membrane blebbing, DNA fragmentation, loss of mitochondrial transmembrane potential and exposure of phosphatidylserine. In addition, the existence of a single mitochondria that is essential for the metabolism and energy production of kinetoplastids also makes it a therapeutic target to investigate [18,19]. Furthermore, it has been demonstrated that trypanosomatids under stress conditions, such as lack of nutrients or drug treatment, can develop an autophagic genotype with the appearance of myelin-like structures, autophagy vacuoles and the intervention of ATG homologs (key proteins in autophagy). Autophagy seems to be a survival strategy of parasites under difficult conditions, it plays a key role in the differentiation processes of trypanosomatids in their life cycle, the elimination of damaged structures and organelles and the maintenance of homeostasis, as well as the maintenance of the mitochondrial functionality. If homeostasis is lost and autophagy is exacerbated, autophagic cell death can be induced. Therefore, this type of death may also be a therapeutic target to evaluate and take into account in the development of new drugs against these parasites [20].

Encouraged by the previous work mentioned before that highlight WA as a potent leishmanicidal and trypanocidal agent, and by the expectation of bio-organosilicone in drug design, the present study used twenty-four known silicon ethers synthesized from WA to evaluate their

in vitro leishmanicidal and trypanocidal activity, as well as their cytotoxicity against murine macrophages. Three of the WA analogs exhibited potent antiparasitic activity and were therefore selected for further testing. Their activity against the intracellular amastigote form of *Leishmania amazonensis* was evaluated, as well as the evaluation of induced physiological changes in the parasites.

2. Materials and methods

2.1. Preparation of silyl ether derivatives from WA

The twenty-four silyl ether derivatives from WA were synthesized by the Quimioplan laboratory at the Instituto Universitario de Bio-Orgánica Antonio González of the University of La Laguna, as described in the previous study by Perestelo et al. [12]. The obtained withanolides were then dissolved in dimethyl sulfoxide (DMSO) (Merck, Darmstadt, Germany) reaching a concentration of 10 mg/ml. The silyl ether derivatives were stored at − 20ºC.

2.2. Biological cultures

For leishmanicidal and trypanocidal activity assays, *L. amazonensis* promastigotes (MHOM/BR/77/LTB0016) were grown in Schneider medium (Sigma-Aldrich, Madrid, Spain) supplemented with 10% fetal bovine serum (VWR, Biowest, Nuaillé, France) and in RPMI 1640 medium (Gibco, Thermo Fisher, Madrid, Spain) with or without phenol red, incubated at 26ºC. Liver Infusion Tryptose (LIT) medium supplemented with 10% fetal bovine serum was used to culture epimastigotes of *T. cruzi* (Y strain) incubated at the same temperature. To maintain the murine macrophage cell line J774A.1 (ATCC TIB-67) Dulbecco's Modified Eagle Medium (Gibco, Thermo Fisher, Madrid, Spain) supplemented with 10% fetal bovine serum was used and they were incubated at 37ºC in 5% CO_2 atmosphere.

2.3. Leishmanicidal and trypanocidal activity assay

To calculate the Inhibitory Concentration 50 (IC_{50}) of the withanolides in each of the parasites tested, a colorimetric assay based on alamarBlue® was performed as previously described by Núñez et al. [21]. For this assay, serial dilutions of the 24 compounds were prepared in sterile 96-well plates using RPMI without phenol red for *L. amazonensis* and LIT for *T. cruzi*. Miltefosine and benznidazole were used as reference drugs. Subsequently, parasites were added to a final concentration of 5×10^5 (*L. amazonensis*) or 2.5×10^5 (*T. cruzi*). Finally, 10% of alamarBlue® was added to each well and incubated for 72 h at 26ºC. Fluorescence was then read using the EnSpire® Multimode Plate Reader (Perkin Elmer, Madrid, Spain). A non-linear regression analysis with 95% confidence limits was employed to calculate IC_{50} values.

2.4. Leishmanicidal activity against amastigotes stage of Leishmania amazonensis

The activity assay against the intracellular form of *L. amazonensis* was also carried out using the alamarBlue® colorimetric assay as described by Bethencourt-Estrella et al. [22]. For this purpose, murine macrophages (at a concentration of 10^5 macrophages per well) were infected with the 7 days-old promastigote culture at 1:10 ratio (macrophage:promastigotes). They were incubated 24 h at 37ºC with 5% CO_2 to achieve optimal infection conditions. Thereafter, the macrophages were washed with RPMI 1640 medium to remove the promastigotes that did not infect the macrophages. Subsequently, these were treated with withanolides for 24 h. Macrophages were ruptured using 0.05% SDS solution for 30 s and incubated at 26 °C for 96 h. Fluorescence was then read using the EnSpire® Multimode Plate Reader (Perkin Elmer, Madrid, Spain). A non-linear regression analysis with 95% confidence limits was employed to calculate IC_{50} values.

2.5. Cytotoxicity assay

To calculate the CC_{50} of the withanolides, murine macrophages (10^5 macrophages per well) are incubated with serial dilutions of the compounds in RPMI 1640 without phenol red. 10% of alamarBlue® was added to each well and incubated at 37 °C in 5% CO_2 atmosphere for 24 h. Finally, fluorescence was measured using the EnSpire® Multimode Plate Reader (Perkin Elmer, Madrid, Spain) and CC_{50} calculated by non-linear regression with 95% confidence limits.

2.6. Study of the mechanism of cell death in the parasites

To determine the mechanisms of cell death induced by the withanolides on the parasites, different experiments were carried out. In all of them it is necessary to incubate the promastigotes of *L. amazonensis* or epimastigotes of *T. cruzi* with the IC_{90} of the withanolides at 26ºC for 24 h. Subsequently, parasites were centrifuged for 10 min at 1500 rpm and the pellet was resuspended in RPMI 1640 without phenol red.

2.6.1. Analysis of ATP levels

To analyze changes in ATP levels on the parasites, CellTiter-Glo® Luminescent Cell Viability Assay (Promega, WI, USA) was added to treated parasites in a white 96-well plate following the manufacturer's instructions. The kit reagent produces cell lysis and emits a luminescence signal which is proportional to the ATP levels produced in the parasites. Afterwards, the luminescence was read using an EnSpire® Multimode Plate Reader (PerkinElmer, Madrid, Spain) as previously described by López-Arencibia et al. [23]. A negative control was added to each experiment (parasites without any treatment) and sodium azide (SIGMA) 20 mM was used as positive control.

2.6.2. Analysis of mitochondrial membrane potential

In order to analyze variations in mitochondrial membrane potential, JC-1 Mitochondrial Membrane Potential Assay Kit® (Cayman Chemical, Ann Arbor, MI, USA) was added to parasites previously treated with withanolides in a black 96-well plate. The reagent of the kit is in dimer form emitting red fluorescence when the mitochondrial membrane potential is under normal conditions, however, when the mitochondrial membrane potential is altered the reagent forms monomers that emit green fluorescence. To measure these fluorescence changes (ratio 595/535 nm) an EnSpire® Multimode Plate Reader (PerkinElmer, Madrid, Spain) is used as previously described by Cartuche et al. [24]. Parasites without treatment were used as negative control and carbonyl cyanide 3-chlorophenylhydrazone (CCCP) 100 μM, (98%, Thermo Scientific™) was added as positive control.

2.6.3. Analysis of plasma membrane permeability

SYTOX® Green nucleic acid stain fluorescent dye (ThermoFisher Scientific, MA, USA) was used to determine changes in cytoplasmic membrane permeability according to the manufacturer's instructions. This green dye only penetrates cells with altered plasma membrane permeability and binds to DNA, multiplying its fluorescence up to 500-fold. EVOS® FL M5000 Cell Imaging System (ThermoFisher Scientific, MA, USA) was used to take pictures after 15 min of incubation [25]. Relative fluorescence intensities were included in a box & whiskers graph. These values were obtained using 40X images and the quantification tools of the EVOS®FL M5000 Cell Imaging System following the manufacturer instructions. Analysis of variance was determined by one-way ANOVA using GraphPad.PRISM® 9.0 software. Significance differences when comparing different percentages values are represented like NS non-significant; *$p < 0.1$; * * $p < 0.01$; * ** $p < 0.001$ and * ** * $p < 0.0001$.

2.6.4. Chromatin condensation determination

Vybrant® Apoptosis Assay Kit n°5, Hoechst 33342/Propidium Iodide (ThermoFisher Scientific, MA, USA) was used following the

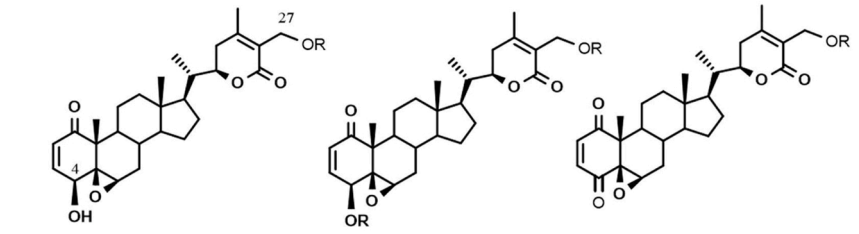

1 R= H **7** R= DMOS **12** R= DMPS **14** R= H **20** R= DMIPS
2 R= TES **8** R= DMVS **13** R= DMOS **15** R= TMS **21** R= DMOS
3 R= TPRS **9** R= MDPS **16** R= TES **22** R= DMVS
4 R= TBS **10** R= TBDMS **17** R= TPRS **23** R= DMPS
5 R= THS **11** R= TBDPS **18** R= TIPS **24** R= MDPS
6 R= DMIPS **19** R= TBS **25** R= TBDMS

TES: tiethylsilyl; **TPRS**: tripropylsilyl; **TBS**: tributylsilyl; **THS**: trihexylsilyl; **DMIPS**: dimethyl-*iso*-propylsilyl; **DMOS**: dimethyloctylsilyl; **DMVS**: dimethylvinylsilyl; **MDPS**: methyldiphenylsilyl; **TBDMS**: *tert*-butyldimethylsilyl; **TBDPS**: *tert*-butyldiphenylsilyl; **DMPS**: dimethylphenylsilyl; **TMS**: trimethylsilyl; **TIPS**: tri-*iso*-propylsilyl

Scheme 1. Structure of Withaferin A-Silyl Ether Analogs.

Table 1
Activity expressed as IC_{50} and selectivity index of withanolides **1–25** against the promastigote stage of *Leishmania amazonensis*, epimastigote stage of *T. cruzi* and cytotoxicity against eukaryotic cells.

Sample	*L. amazonensis*		*T. cruzi*		*J774A.1*
	IC_{50}[a]	SI[b]	IC_{50}[a]	SI[b]	CC_{50}[c]
1	0.83 ± 0.07	14.4	1.02 ± 0.10	11.7	11.92 ± 1.08
2	0.55 ± 0.14	15.6			8.51 ± 1.33
4	0.55 ± 0.12	17.4	2.39 ± 0.70	4.0	9.57 ± 0.64
7	0.44 ± 0.03	21.3	5.87 ± 0.23	1.6	9.31 ± 0.89
8	1.08 ± 0.14	10.8	2.94 ± 0.40	4.0	11.62 ± 1.73
10	0.19 ± 0.01	65.3	0.14 ± 0.01	88.6	12.40 ± 1.88
12	0.39 ± 0.09	72.6	1.93 ± 0.27	14.7	28.32 ± 2.14
15	0.78 ± 0.07	16.8	5.08 ± 0.81	2.6	13.26 ± 0.48
17	0.83 ± 0.10	14.6	3.30 ± 0.34	3.7	12.08 ± 2.69
18	1.90 ± 0.08	6.8	3.74 ± 0.08	3.5	12.93 ± 0.85
20	0.47 ± 0.07	15.7	1.41 ± 0.05	5.4	7.38 ± 1.84
22	2.77 ± 0.01	4.2	4.54 ± 0.15	2.6	11.58 ± 0.36
24	1.10 ± 0.11	3.6			4.00 ± 0.33
25	0.75 ± 0.03	5.2	0.89 ± 0.02	4.4	3.91 ± 0.32
M[d]	6.48 ± 0.10	11.1			72.18 ± 1.25
B[d]			6.95 ± 0.50	57.5	399.91 ± 1.04

[a] IC_{50}: concentrations able to inhibit 50% of parasites after 72 h, expressed as μM ± standard deviation (SD).
[b] SI: selectivity index (CC_{50}/IC_{50}).
[c] CC_{50} concentration able to inhibit 50% of murine macrophages after 24 h, expressed as μM ± standard deviation (SD).
[d] M: miltefosine and B: benznidazole were used as the positive controls against *L. amazonensis* and *T. cruzi*, respectively.

manufacturer's instructions to determine the chromatin condensation in the treated parasites. Hoechst 33342 dye binds to the condensed chromatin and emits intense blue fluorescence. Propidium iodide (PI) penetrates the dead cells and binds to their DNA emitting red fluorescence. Therefore, up to three types of cell populations can be recognized: living cells (show soft blue fluorescence); cells undergoing programmed cell death (PCD) (strong blue fluorescence) and dead cells (high red fluorescence). After incubating the parasites treated with Hoechst 33342 at 5 μg/ml and PI at 1 μg/ml as previously described Díaz-Marrero et al. [26], pictures were taken using the EVOS® FL M5000 Cell Imaging System (ThermoFisher Scientific, MA, USA). Relative fluorescence intensities were included in a box & whiskers graph. These values were obtained using 40X images and the quantification tools of the EVOS®FL M5000 Cell Imaging System following the manufacturer instructions. Analysis of variance was determined by one-way ANOVA using GraphPad.PRISM® 9.0 software. Significance differences when comparing different percentages values are represented like NS non-significant; *p < 0.1; * * p < 0.01; * ** p < 0.001 and * ** * p < 0.0001.

2.6.5. Analysis of reactive oxygen species

To measure the accumulation of reactive oxygen species (ROS) inside the treated parasites, CellROX® Deep Red Reagent (ThermoFisher Scientific, MA, USA) was used at a concentration of 5 μM during 30 min of incubation at 26 °C, following the manufacturer's instructions. EVOS® FL M5000 Cell Imaging System (ThermoFisher Scientific, MA, USA) was used to take pictures of the parasites. Red fluorescence indicates the presence of reactive oxygen species [27]. Relative fluorescence intensities were included in a box & whiskers graph. These values were obtained using 40X images and the quantification tools of the EVOS®FL M5000 Cell Imaging System following the manufacturer instructions. Analysis of variance was determined by one-way ANOVA using GraphPad.PRISM® 9.0 software. Significance differences when comparing different percentages values are represented like NS non-significant; *p < 0.1; * * p < 0.01; * ** p < 0.001 and * ** * p < 0.0001.

2.6.6. Autophagy assay

Monodansylcadaverine (MCD) is an autofluorescent dye commonly used to determine the presence of autophagic vacuoles [28]. The MCD dye binds to the autophagic membrane vacuoles and emits blue fluorescence. This is possible due to the combination of ion sequestration and the interactions with some specific lipids of the autophagic membrane. After incubation of the parasites with the IC_{90} of selected withanolides and centrifugation, we added MCD dye in darkness conditions at a final concentration of 100 μM. One hour of incubation later, we centrifuged again and added RPMI without phenol red to reduce background. Pictures were taken using EVOS® FL M5000 Cell Imaging System (ThermoFisher Scientific, MA, USA).

Table 2
Previous results of trypanocidal and leishmanicidal activity from literature, in comparison with the current results obtained in the present study.

Parasite	Previous literature			Current results	
	Reference	Compound	IC_{50} (μM)	Compound	IC_{50} (μM)
T. cruzi (epimastigotes)	Nagafuji et al. [35]	Physagulin C	14.00	Withanolide 10	0.14
	López-Arencibia et al. [10]	Witharistatin	2.41	Withanolide 12	1.93
L. amazonensis (promastigotes)	López-Arencibia et al. [10]	Witharistatin	2.82	Withanolide 7	0.44
	Lima et al. [37]	Aurelianolide A	7.60	Withanolide 10	0.19
		Aurelianolide B	7.90	Withanolide 12	0.39
L. major (promastigotes)	Kuroyanagi et al. [33]	Withanolide J	5.70	Not determined	
	Choudhary et al. [34]	16,24-cyclo-13,14-secoergost-2-ene-18,26-dioic acid	1.64		

Table 3
Leishmanicidal activity of withanolides **1**, **4**, **7**, **10**, **12**, and **15** against the amastigote stage of *Leishmania amazonensis* and cytotoxicity against eukaryotic cells.

Sample	*L. amazonensis*	
	IC_{50}[a]	SI[b]
WA (**1**)	0.06 ± 0.01	198.7
4	0.30 ± 0.02	31.9
7	0.12 ± 0.00	77.6
10	0.31 ± 0.01	40.0
12	0.47 ± 0.02	60.3
15	0.80 ± 0.12	16.6
M[c]	3.12 ± 0.12	23.1

[a] IC_{50}: concentrations able to inhibit 50% of parasites after 24 h, expressed as μM ± standard deviation (SD).
[b] SI: electivity index (CC_{50}/IC_{50}).
[c] M: miltefosine was used as the positive control against *L. amazonensis*.

2.7. Statistical analysis

All assays are performed three times on different days. The IC_{50} and CC_{50} were calculated using Sigma Plot 12.0 statistical analysis software (Systat Software) by non-linear regression with 95% confidence limits. Results are expressed as the mean of the three replicates ± standard deviation. Plots of ATP and mitochondrial membrane potential results are made using GraphPad.PRISM® 9.0 software program (GraphPad Software, San Diego, CA, USA). Analysis of variance was determined by one-way ANOVA. Differences of $p < 0.05$ were considered statistically significant.

3. Results and discussion

The *in vitro* anti-kinetoplastid activity of lead compound **1**, derivative **14** (4-oxo-WA) and their silyl analogs **2**-**13** and **15**-**25** was evaluated on promastigotes and amastigotes stages of *leishmania amazonensis* and epimastigotes of *Tripanosoma cruzi.* Cytotoxicity was also determined in a normal eukaryotic cell line (Murine macrophages *J7741A.1*) to test selectivity (Scheme 1). Miltefosine and benznidazole were used as reference drugs for leishmanicidal and trypanocidal activity, respectively (Table 1).

In general, the studied withanolides showed promising leishmanicidal and trypanocidal activity, being in most cases even higher than the antiparasitic activity shown by the reference drugs (miltefosine and benznidazole). Compounds **3**, **5** and **6** showed dissolution difficulties. Furthermore, they were not active against any of the parasites tested. Compounds **11**, **13**, **14**, **16**, **19**, **21** and **23** showed high toxicity against murine macrophages (data not shown), therefore antiparasitic activity assays were not continued. Although some withanolides were slightly toxic in macrophages, the obtained results were interesting from the selectivity indices point of view. These indices showed that silicon ethers synthesized from WA are promising candidates as potential antiparasitic treatments against *L. amazonensis* and *T. cruzi*. The activity of the compounds was also evaluated against another strain of *Leishmania*:

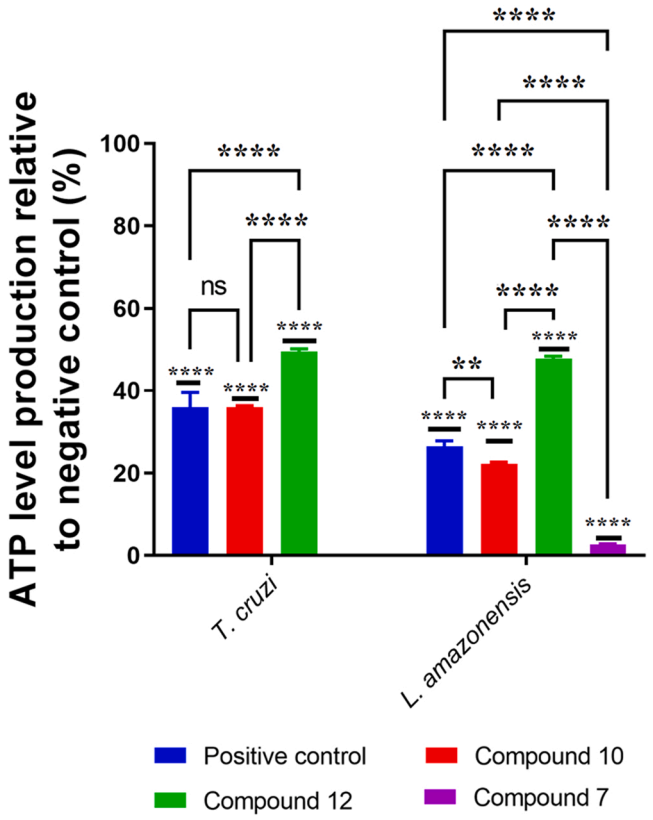

Fig. 1. Percentage of ATP level relative to negative control. Sodium azide was used as a positive control at a concentration of 20 mM. Analysis of variance was determined by one-way ANOVA using GraphPad.PRISM® 9.0 software. Significance differences when comparing different percentages values are represented like ns = non-significant; *$p < 0.1$; ** $p < 0.01$; *** $p < 0.001$ and **** $p < 0.0001$.

L. donovani. Although most of these withanolides showed high activity levels on this parasite (data not shown), the activity/cytotoxicity ratio did not show good selectivity, thus the antiparasitic activity of silicon ethers synthesized from WA against this *Leishmania* species was not further studied.

Comparing these results with those found in the literature, the obtained results support the important biological activity demonstrated by withanolides in previous studies. The recent review by Singh et al. [29] has collected data from other studies on several withanolides isolated from different plant genera such as *Physalis* and *Withania* (among others), as well as synthetic withanolides, which showed different biological activities. For instance, Lin et al. reported the anti-inflammatory activity of withanolides from *Physalis minima* [30] and Nicolas et al. isolated withanolides from *Nicandra john-tyleriana* with antibacterial activity [31]. In another study Xia et al. isolated withanolides from *P. pubescens* and reported their anticancer activity against eight human

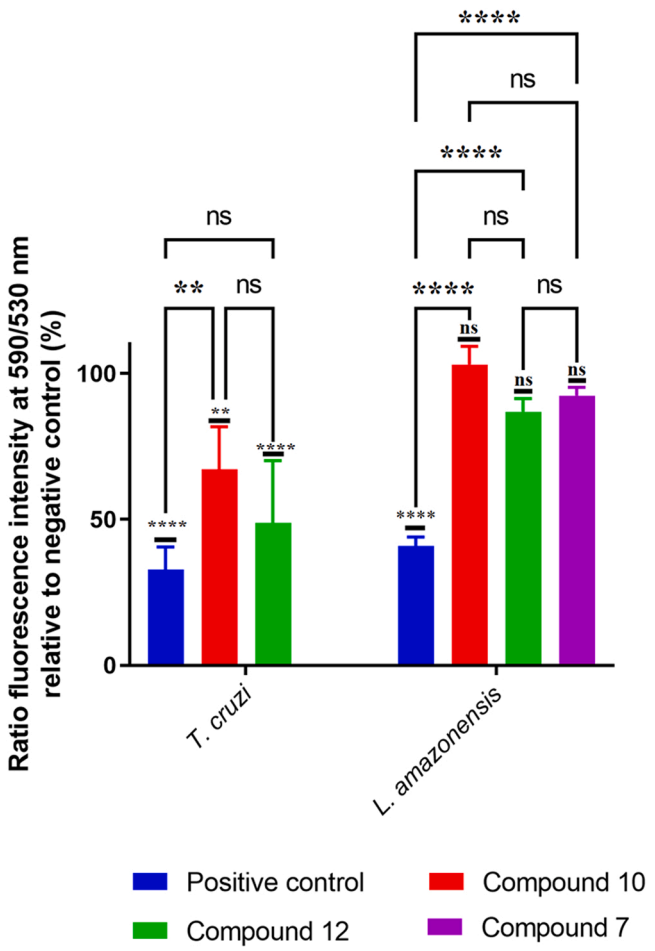

Fig. 2. Percentage relative to negative control of ratio fluorescence intensity at 590/530 nm. CCCP was used as a positive control at a concentration of 100 μM. Analysis of variance was determined by one-way ANOVA using GraphPad. PRISM® 9.0 software. Significance differences when comparing different percentages values are represented like NS non-significant; *p < 0.1; ** p < 0.01; *** p < 0.001 and **** p < 0.0001.

tumor cell lines [32]. Furthermore, the leishmanicidal activity of new withanolides from *Withania coagulans* against *L. major* was demonstrated by Kuroyanagi et al. [33].

In a previous work by López-Arencibia et al. [10], an acetone extract was obtained from the leaves of the plant *Withania aristata.* In addition, their leishmanicidal and trypanocidal activity was evaluated showing promising results, so bioguided fractionation was continued to isolate three pure compounds, or withanolides: WA, 4β,17α,27-trihydroxy-1-oxo-witha-2,5,24-trienolide and witharistatin. These compounds, especially WA, showed superior leishmanicidal and trypanocidal activity compared to the reference drugs miltefosine and benznidazole. In addition, the results obtained in the present study also confirmed the previously reported leishmanicidal and trypanocidal potential of withanolides.

Taking into account these previous results from López-Arencibia et al. [10], in subsequent work by Perestelo et al. [12], 34 compounds were synthesized from WA by incorporating silicon into the molecular structures with the aim of improving their therapeutic potential. In this study, these compounds also were reported to present potent antitumor activity in human ovarian carcinoma cells (IC_{50} values from 1.5 to 59 nM in A2780 cell lines).

Anti-kinetoplastid activity on *T. cruzi* epimastigotes indicated that analogs **4**, **8**, **10**, **12**, **17**, **18**, **20**, **22**, and **25** were 1.5–49.6-fold more potent (IC_{50} ranging from 4.54 to 0.14 μM) than reference drug (benznidazole, IC_{50} 6.95 μM) (Table 1). Moreover, these compounds had a selectivity index ranging from good to excellent for the *Trypanosoma* strain. Only compound **10** was more potent than the lead compound WA (**1**), with a high selectivity index (SI > 88). Previous studies have also demonstrated the trypanocidal activity of some withanolides that are different from those tested in this study (Table 2). The best compound from the references cited and the best compounds from this study are listed in the table. Nagafuji et al. [35] isolated 10 withanolides from *P. angulata* and tested their trypanocidal activity against *T. cruzi* epimastigotes and trypomastigotes. These withanolides were found to be more active on trypomastigotes than on epimastigotes, demonstrating their high potential in Chagas chemotherapy. In this research, the withanolide with the best IC_{50} against the epimastigotes of this parasite presented an activity value of 14 μM, while the values obtained in the present study were lower than 5.87 μM. Even compound **10** showed an IC_{50} value of 0.14 μM. Therefore, it seems that synthesized silicon ethers from WA possess better trypanocidal activity than reported so far in the literature.

The results of *in vitro* assays against the *L. amazonensis* promastigotes revealed that the activity of 13 analogs (compounds **2**, **4**, **7**, **8**, **10**, **12**, **15**, **17**, **18**, **20**, **22**, **24** and **25**) was higher than that of the widely known reference drug (miltefosine), with IC_{50} values ranging from 2.77 to 0.19 μM (Table 1). Moreover, six compounds of them (**2**, **4**, **7**, **10**, **12**, and **20**) were more potent than the lead compound WA (**1**). After confirming that some of the analogs showed potent leishmanicidal activity, cytotoxicity was evaluated against a normal cell line to test their selectivity (Table 1). According to Suffness et al. [36] a selectivity index (SI) value superior to two indicates good selectivity. All 13 analogs showed good selectivity with SI values ranging from 3.6 to 72.6. Notably, dimethyl tert-butyl silyl ether analog **10** (IC_{50} 0.19 μM) showed favorable trends for optimal leishmanicidal activity. This WA analog improved the profile 4.4-fold over lead compound **1**. In addition, compound **10** was approximately 34-fold more active than miltefosine and showed markedly lower cytotoxicity in the murine macrophage cell line (SI > 65). According to the literature (Table 2), there are numerous studies demonstrating the leishmanicidal activity of withanolides. All results reported in the literature are based on withanolides isolated from natural plants. No studies of antiparasitic activity on synthetic WA analogs were found. Kuroyanagi et al. [33] isolated 11 withanolides from *W. coagulans* that showed good activity against *L. major* promastigotes, with IC_{50} values up to 5.7 μM. Lima et al. [37] successfully purified two withanolides (Aurelianolide A and B) from *Aureliana fasciculata* demonstrating potent leishmanicidal activity on *L. amazonensis* promastigotes (IC_{50} values of 7.6 and 7.9 μM, respectively). However, the literature consulted has not shown better results than those obtained in this study for withanolides synthesized from WA (Table 2).

Based on the *in vitro* results obtained on *L. amazonensis* promastigotes and *T.cruzi* epimastigotes, analogs **4**, **7**, **10**, **12** and **15** were selected for further studies on the intracellular amastigote stage of *L. amazonensis* (Table 3). Anti-kinetoplastid activity revealed that all silyl-withanolides were more potent against amastigotes than the miltefosine (IC_{50} 3.12 μM). These compounds showed promising IC_{50} values ranging from 0.12 to 0.8 μM. Moreover, all four compounds showed a higher selectivity index than miltefosine. In fact, analog **7** was 26-fold more potent than the reference drug (Table 3), with an SI of 77.6 *versus* 23.1 for miltefosine. However, all of them were less active against the amastigote form than the lead compound, WA. The promising results obtained in this study against the intracellular form of *L. amazonensis* are confirmed by comparison with results obtained in other studies in the literature. For instance, Lima et al. demonstrated the activity against *L. amazonensis* amastigotes of the withanolides Aurelianolide A and B with IC_{50} values much higher than those of the present study (IC_{50} of 2.3 and 6.4 μM, respectively) [37].

On the other hand, compounds **4, 10**, **12** and **15** have also demonstrated antitumor activity in human ovarian carcinoma cells [12], but their promising leishmanicidal and trypanocidal activity has not been

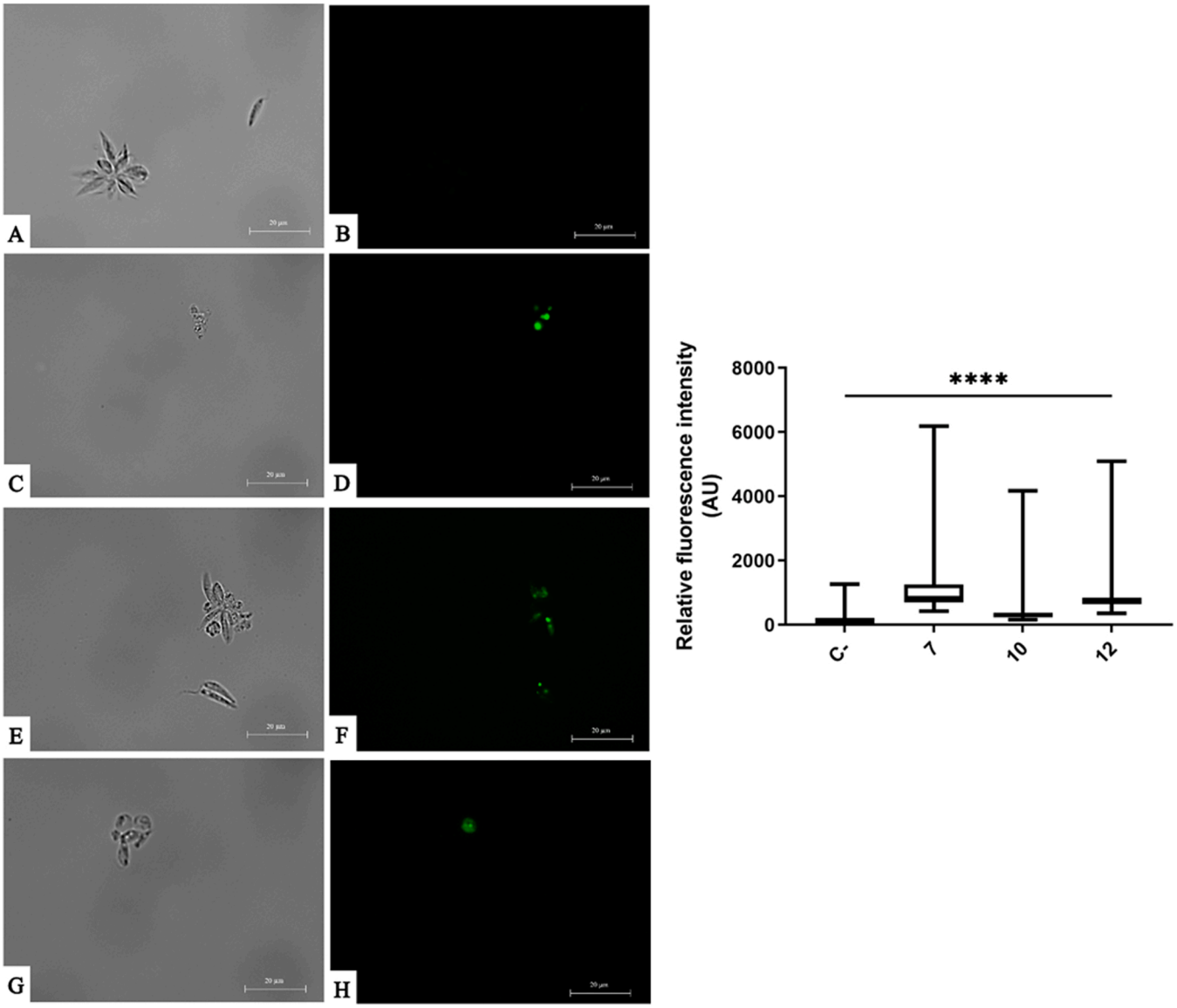

Fig. 3. *L. amazonensis* promastigotes incubated with IC_{90} withanolide **10** (C,D), withanolide **12** (E,F) and withanolide **7** (G,H) during 24 h. Negative control of the parasites without any treatment (A,B). The 100X images were captured using an EVOS® FL M5000 Cell Imaging System. Scale-bar: 20 μm. The box & whiskers graph includes the relative fluorescence intensities. These values were obtained using 40X images and the quantification tools of the EVOS®FL M5000 Cell Imaging System following the manufacturer instructions. Analysis of variance was determined by one-way ANOVA using GraphPad.PRISM® 9.0 software. Significance differences when comparing different percentages values are represented like NS non-significant; *$p < 0.1$; ** $p < 0.01$; *** $p < 0.001$ and **** $p < 0.0001$.

reported so far in the literature.

Considering their efficacy against *L. amazonensis* promastigotes, *T. cruzi* epimastigotes, *L. amazonensis* amastigotes, as well as their remarkable low cytotoxicity, compounds **7**, **10** and **12** were selected for further studies to elucidate their mechanism of action.

As a next step, it was necessary to evaluate the mechanism of action of these compounds at the cellular level in *L. amazonensis* and *T. cruzi*. In order to determine whether these compounds induce programmed cell death (PCD) in the parasites, different assays were carried out.

3.1. ATP level analysis

To determine the mitochondrial damage caused by these withanolides in the parasites, the first assay was to determine the changes induced in the mitochondrial ATP levels. For this purpose, parasites were incubated for 24 h with IC_{90} of the compounds and the Cell Titer-Glo® Luminescent Cell Viability Assay kit (Promega, WI, USA) was used according to the manufacturer's instructions. The results are shown in Fig. 1. Analysis of variance was performed by one-way ANOVA. For *T. cruzi*, withanolides **10** and **12** significantly decreased mitochondrial ATP levels by about 50% compared to untreated cells. Similar effects occur with withanolides **7**, **10**, and **12** in the case of *L. amazonensis*. Withanolide **7** caused the greatest changes in mitochondrial ATP levels in this parasite, reaching levels close to 5% when compared to untreated, followed by withanolide **10** (20%) and withanolide **12** (50%).

3.2. Analysis of mitochondrial membrane potential changes

The effect of withanolides on the mitochondrial membrane potential of the parasites was studied using the fluorophore JC-1 according to the manufacturer's recommendations. For this, parasites were incubated for 24 h with IC_{90} of the compounds and after adding the reagent, the two fluorescences were measured. The analysis of variance of the data obtained was determined by one-way ANOVA and the results are shown in Fig. 2. In the case of *T. cruzi*, withanolides **10** and **12** induce significant changes in the mitochondrial membrane potential with respect to the

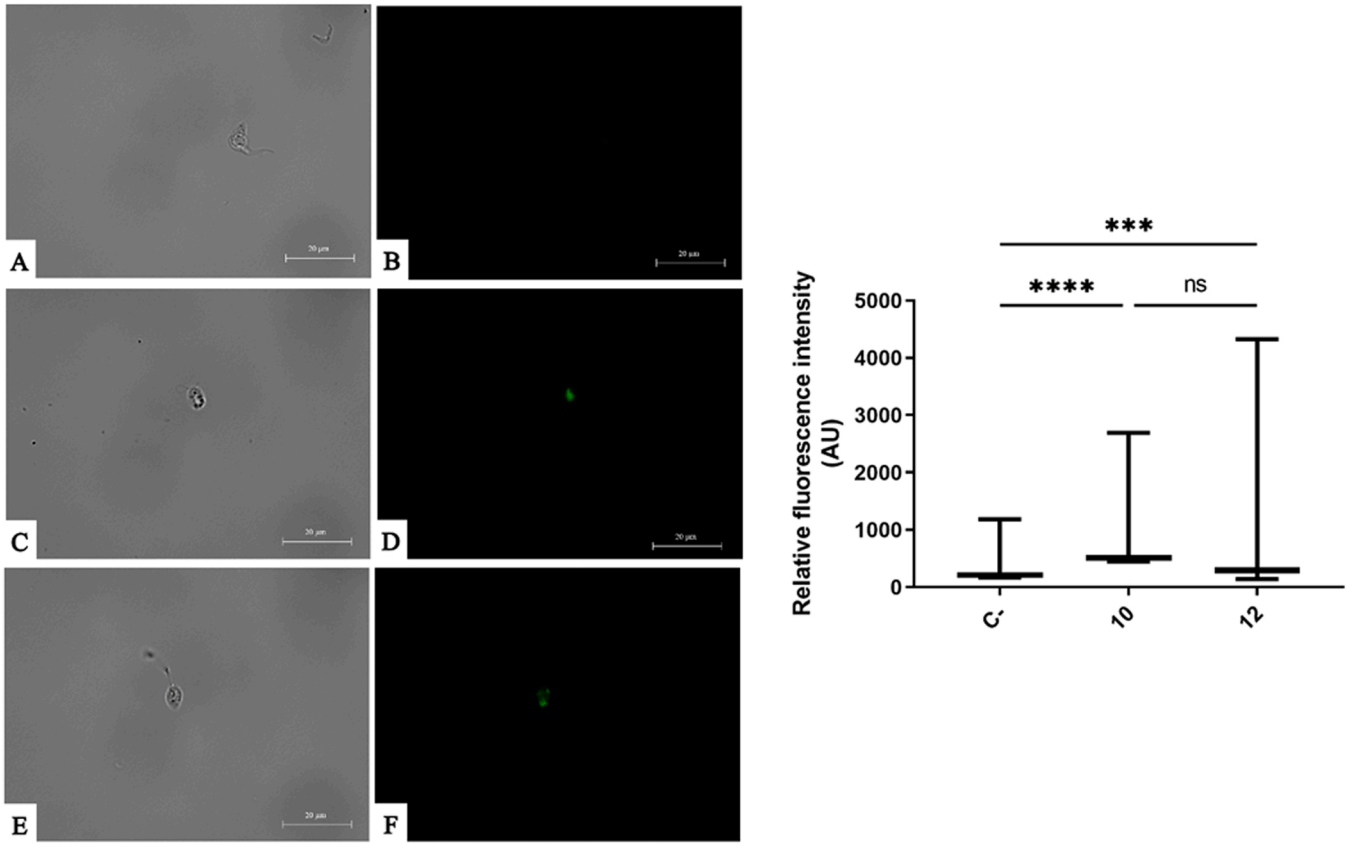

Fig. 4. *T. cruzi* epimastigotes incubated with IC_{90} of withanolide **10** (C,D) and withanolide **12** (E,F) during 24 h. Negative control of the parasite without any treatment (A,B). The 100X images were captured using an EVOS® FL M5000 Cell Imaging System. Scale-bar: 20 μm. The box & whiskers graph includes the relative fluorescence intensities. These values were obtained using 40X images and the quantification tools of the EVOS®FL M5000 Cell Imaging System following the manufacturer instructions. Analysis of variance was determined by one-way ANOVA using GraphPad.PRISM® 9.0 software. Significance differences when comparing different percentages values are represented like NS non-significant; *$p < 0.1$; ** $p < 0.01$; *** $p < 0.001$ and **** $p < 0.0001$.

control, with compound **12** causing the greatest decrease in potential. However, in the case of *L. amazonensis*, withanolides **7**, **10** and **12** did not produce significant changes in mitochondrial membrane potential with respect to the untreated control.

3.3. Plasmatic membrane permeability assay and chromatin condensation analysis

Several studies in the literature have shown that nuclear chromatin condensation, DNA fragmentation and increased membrane permeability, among others, are some of the most characteristic signs of apoptosis in kinetoplastids [18,19].

To determine whether WA-derived compounds cause an increase in membrane permeability, *L. amazonensis* promastigotes and *T. cruzi* epimastigotes were incubated with IC_{90} of the withanolides for 24 h. Subsequently, SYTOX® Green, which emits green fluorescence inside cells with increased plasma membrane permeability, was added to the assay. The results obtained in *L. amazonensis* (Fig. 3) and *T. cruzi* (Fig. 5) show that the withanolides tested seem to induce slight variations in the plasma membrane permeability of all parasites, since it is possible to observe a slight green fluorescence. Remarkably, as can be seen in the transmitted light images, the cell integrity and shape of the parasites is maintained, which would also rule out a necrotic process [20]. Furthermore, the box-and-whisker plot in *L. amazonensis* (Fig. 3) confirms that all withanolides showed significantly higher green fluorescence compared to the control. In addition, the intensity of fluorescence produced by the compounds was also significantly different among them, so that the compounds seem to affect the permeability of the parasite plasma membrane differently.

As for the box-and-whisker plot on *T. cruzi* (Fig. 4), the results also confirm that all withanolides showed significantly higher green fluorescence compared to the control. However, the intensity of the fluorescence produced by the tested compounds was not significantly different among them, so it seems that they cause similar alterations in the permeability of the parasite's plasma membrane.

Following the manufacturer's instructions, parasites were also exposed to the Vybrant® Apoptosis Assay Kit n°5, Hoechst 33342/Propidium Iodide. With this assay it is possible to detect nuclear chromatin condensation by the emission of strong blue fluorescence. In addition, cells showing red fluorescence would indicate that they are in an advanced process of death.

According to the obtained results for *L. amazonensis* (Fig. 5) and *T. cruzi* (Fig. 6), it was clear that chromatin condensation was occurring in both parasites incubated with the withanolides, as they showed intense blue fluorescence localized in the nucleus. In addition, parasitic cells that were visibly more damaged also showed red fluorescence, indicating a more advanced process of death. This could also be confirmed by the results obtained from box-and-whisker plots representing the relative fluorescence intensities of Hoechst 33342 for *L. amazonensis* (Fig. 5) and *T. cruzi* (Fig. 6). These graphs confirm that all withanolides showed significantly higher blue fluorescence compared to the untreated control for both parasites. The fluorescence intensity produced by the tested compounds was also significantly different between them, so the compounds seem to affect chromatin condensation differently.

As for the propidium iodide assay in *L. amazonensis*, although red fluorescence was observed in some parasites in the 100X images, after quantification of this fluorescence with the 40X images, different results

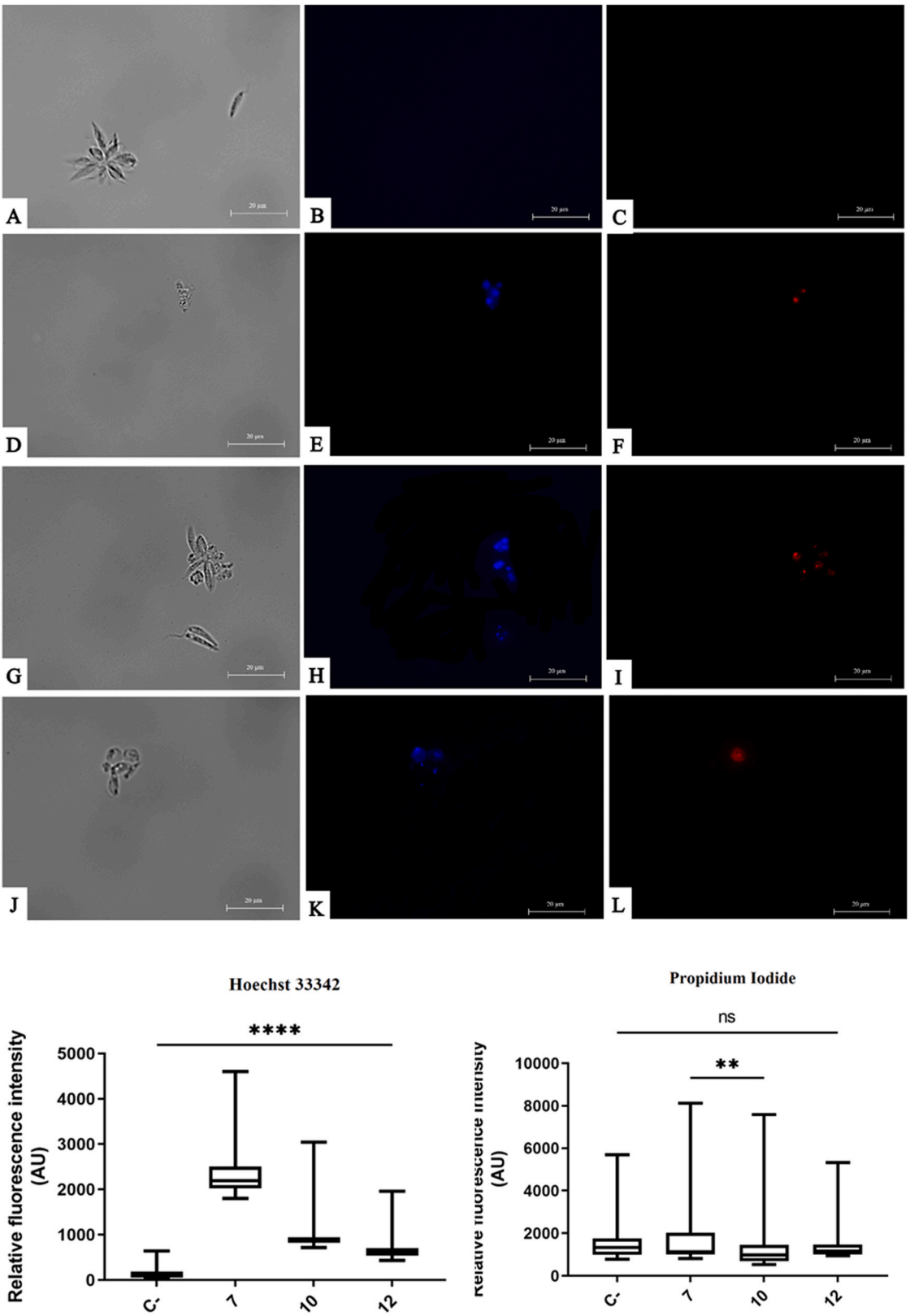

Fig. 5. *L. amazonensis* promastigotes incubated with IC_{90} withanolide **10** (D,E,F), withanolide **12** (G,H,I) and withanolide **7** (J,K,L) during 24 h. Negative control of the parasites without any treatment (A,B,C). The 100X images were captured using an EVOS® FL M5000 Cell Imaging System. Scale-bar: 20 μm. The box & whiskers graph includes the relative fluorescence intensities. These values were obtained using 40X images and the quantification tools of the EVOS®FL M5000 Cell Imaging System following the manufacturer instructions. Analysis of variance was determined by one-way ANOVA using GraphPad.PRISM® 9.0 software. Significance differences when comparing different percentages values are represented like NS non-significant; *$p < 0.1$; ** $p < 0.01$; *** $p < 0.001$ and **** $p < 0.0001$.

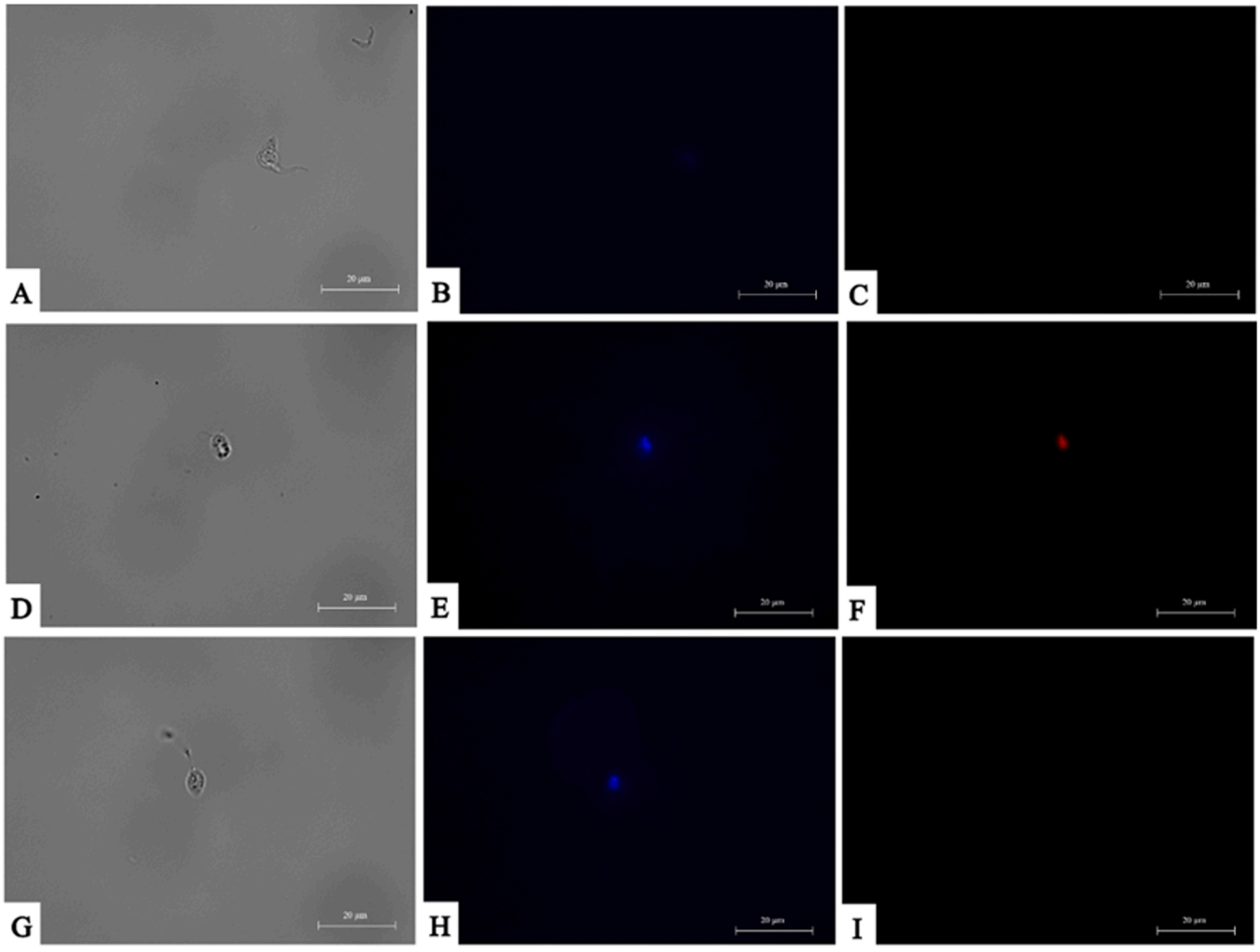

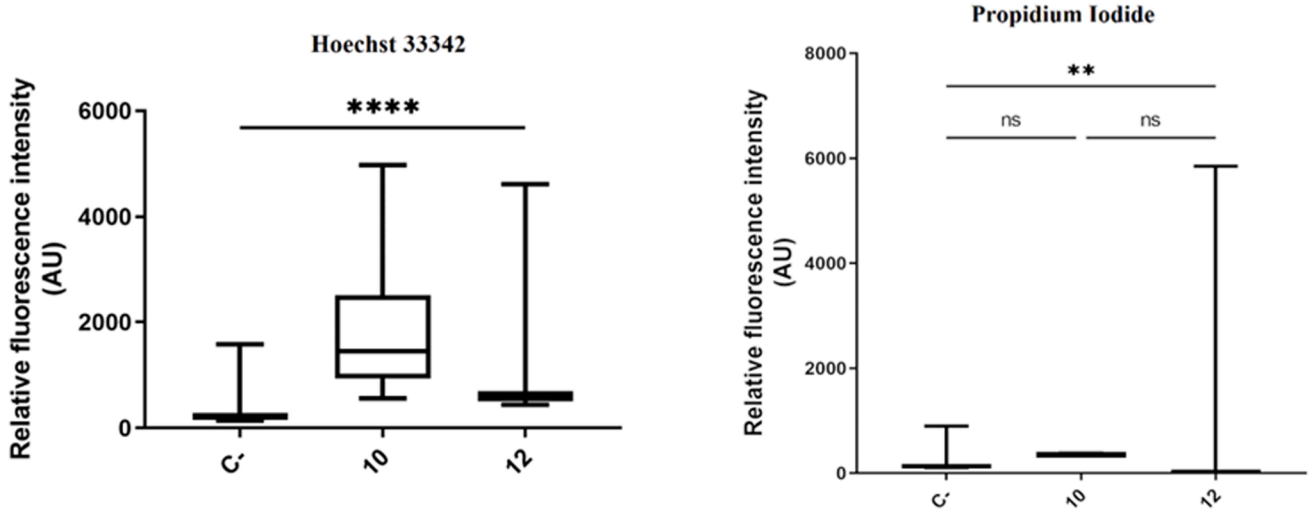

Fig. 6. *T. cruzi* epimastigotes incubated with IC_{90} of withanolide **10** (D,E,F) and withanolide **12** (G,H,I) during 24 h. Negative control of the parasite without any treatment (A,B,C). The 100X images were captured using EVOS® FL M5000 Cell Imaging System. Scale-bar: 20 μm. The box & whiskers graph includes the relative fluorescence intensities. These values were obtained using 40X images and the quantification tools of the EVOS®FL M5000 Cell Imaging System following the manufacturer instructions. Analysis of variance was determined by one-way ANOVA using GraphPad.PRISM® 9.0 software. Significance differences when comparing different percentages values are represented like NS non-significant; *$p < 0.1$; ** $p < 0.01$; *** $p < 0.001$ and **** $p < 0.0001$.

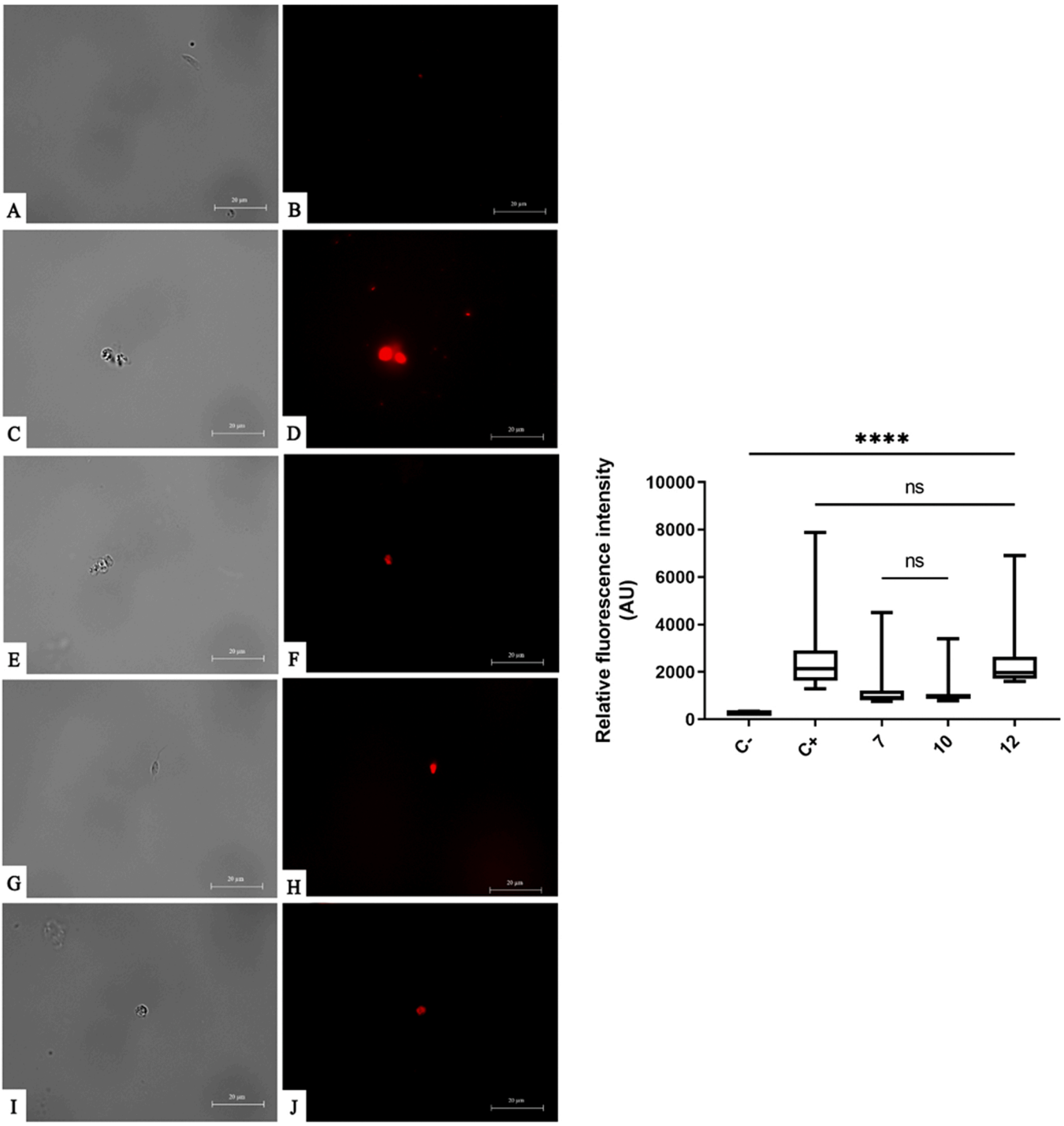

Fig. 7. *L. amazonensis* promastigotes incubated with IC_{90} of withanolide **10** (E,F), withanolide **12** (G,H) and withanolide **7** (I,J) during 24 h. Negative control of the parasite without treatment (A,B) and the positive control with H_2O_2 at 600 μM (C,D). The 100X images were captured using an EVOS® FL M5000 Cell Imaging System. Scale-bar: 20 μm. The box & whiskers graph includes the relative fluorescence intensities. These values were obtained using 40X images and the quantification tools of the EVOS®FL M5000 Cell Imaging System following the manufacturer instructions. Analysis of variance was determined by one-way ANOVA using GraphPad.PRISM® 9.0 software. Significance differences when comparing different percentages values are represented like NS non-significant; *$p < 0.1$; ** $p < 0.01$; *** $p < 0.001$ and **** $p < 0.0001$.

were observed in the graph (Fig. 5). It was confirmed that the compounds showed no significant difference in red fluorescence compared to the control. Therefore, withanolides induce chromatin condensation in *L. amazonensis* without evidence of an advanced cell death process.

Regarding the box-and-whisker plot of *T. cruzi* (Fig. 6) for the propidium iodide assay, some differences are observed between the 100X images and the results of the plot. This is because only a few parasites are observed in the 100X images, however quantification of fluorescence using the 40X images, where there are a larger number of parasites, allowed us to obtain more representative results. In relation to this, the graph showed that withanolide **10** did not show significant differences in red fluorescence with respect to the control Hence, this compound seems to be inducing the early stages of cell death in the parasite. However, withanolide **12** showed a significantly higher red fluorescence

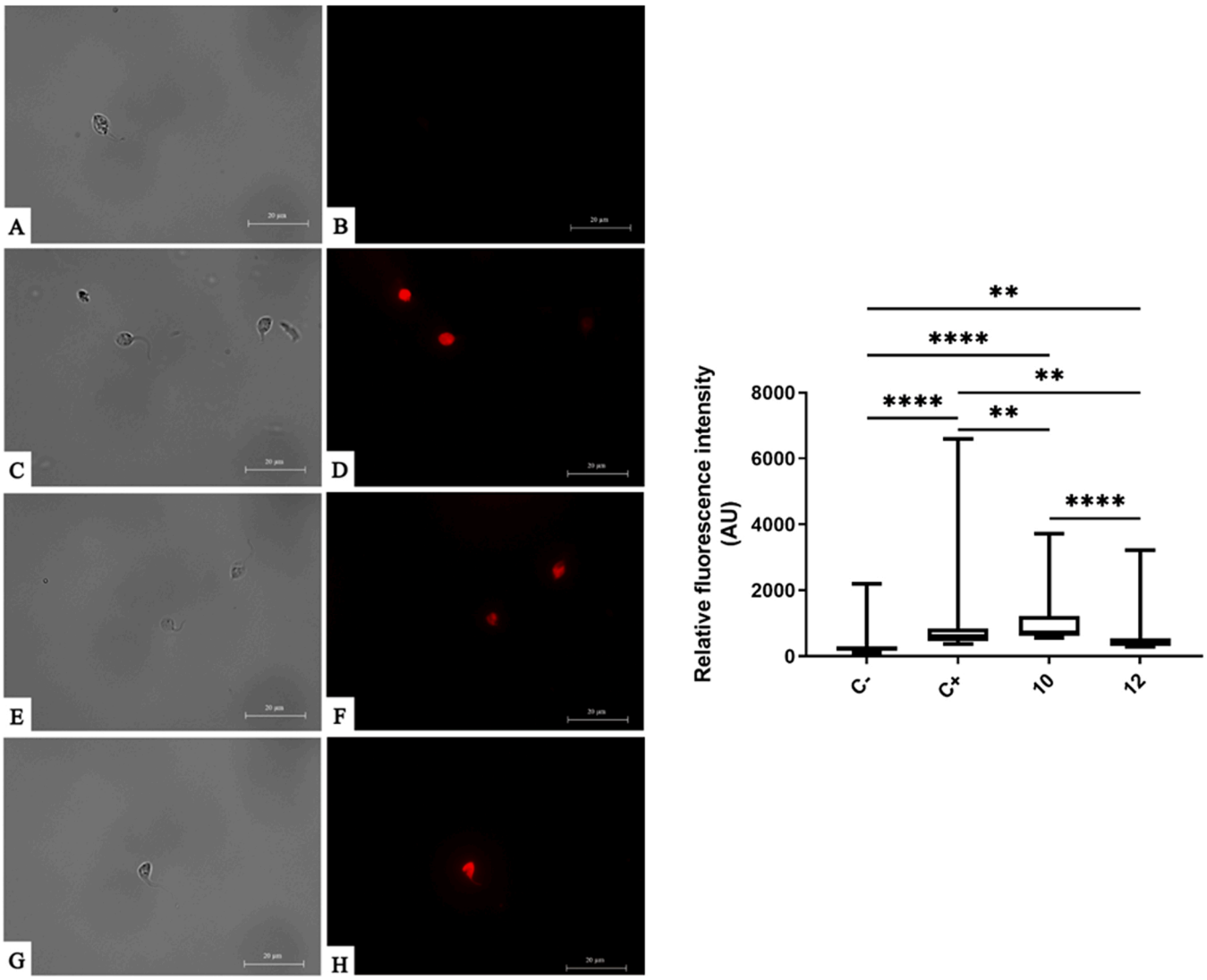

Fig. 8. *T. cruzi* epimastigotes incubated with IC_{90} of withanolide **10** (E,F) and withanolide **12** (G,H) during 24 h. Negative control of the parasite without treatment (A,B) and the positive control with H_2O_2 at 600 μM (C,D). The 100X images were captured using an EVOS® FL M500 Cell Imaging System. Scale-bar: 20 μm. The box & whiskers graph includes the relative fluorescence intensities. These values were obtained using 40X images and the quantification tools of the EVOS®FL M5000 Cell Imaging System following the manufacturer instructions. Analysis of variance was determined by one-way ANOVA using GraphPad.PRISM® 9.0 software. Significance differences when comparing different percentages values are represented like NS non-significant; *$p < 0.1$; ** $p < 0.01$; *** $p < 0.001$ and **** $p < 0.0001$.

than the control, indicating that this compound induces cell death more rapidly in *T. cruzi*, so the parasites are in a more advanced stage of death.

3.4. Analysis of reactive oxygen species

As illustrated in Figs. 7 and 8, *L. amazonensis* promastigotes and *T. cruzi* epimastigotes incubated with IC_{90} of the selected withanolides for 24 h showed intense red fluorescence. This is because the parasites have been exposed to the CellROX® Deep Red Reagent assay, which is indicating that an accumulation of reactive oxygen species (ROS) is occurring inside the parasites. This accumulation of ROS is a well-known signal that occurs before programmed cell death develops [18]. The presence of ROS in the parasites was also confirmed by the relative fluorescence intensities depicted in the graphs in Figs. 7 and 8. These graphs confirm that all withanolides showed significantly higher red fluorescence compared to the negative control for both parasites. The intensity of the fluorescence produced by the tested compounds was also significantly different between them, so the compounds seem to affect the accumulation of reactive oxygen species differently. The intensity of red fluorescence was not significantly different between withanolides **7** and **10** in the case of *L. amazonensis*. Therefore, these two compounds seem to induce a similar levels of ROS accumulation in the treated cells.

3.5. Monodansyl cadaverine

The formation of autophagic vacuoles, in parasites incubated with IC_{90} of the selected withanolides for 24 h, was assessed by the Monodansyl cadaverine (MCD) assay. With this fluorophore, parasites with autophagic vacuoles will show an intense blue fluorescence in their cytoplasm corresponding to the abovementioned vacuoles. The results obtained for *L. amazonensis* (Fig. 9) and *T. cruzi* (Fig. 10) showed that the selected withanolides induce the formation of autophagic vacuoles in both parasites (indicated with arrows in the figures), as a strong blue fluorescence in the form of vesicles can be observed in both treated promastigotes of *L. amazonensis* and epimastigotes of *T. cruzi*.

Overall, these results demonstrated that silicon ethers synthesized from WA are promising molecules in the development of new leishmanicidal and trypanocidal drugs. In fact, previous studies had already

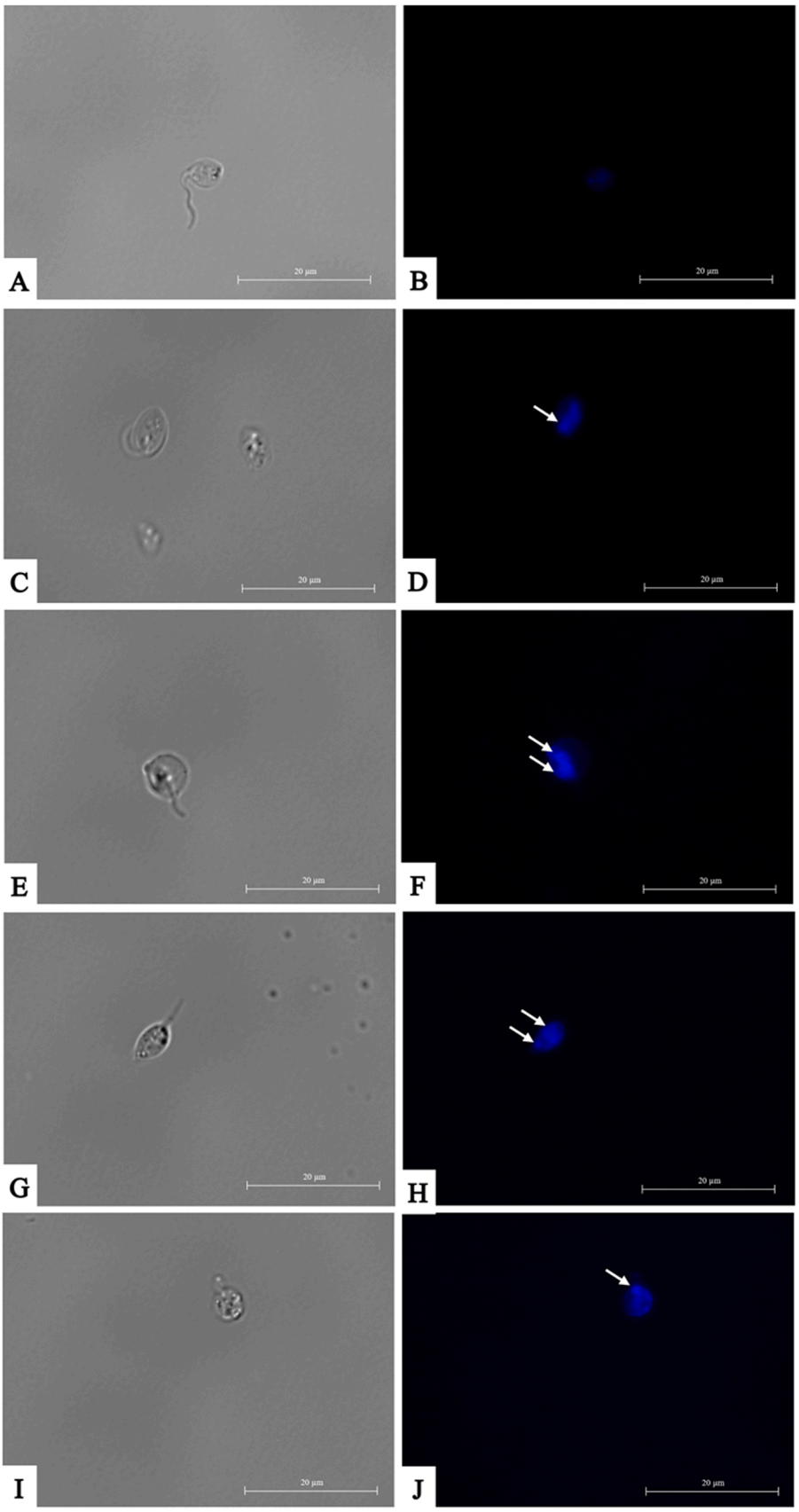

Fig. 9. *L. amazonensis* promastigotes incubated with IC_{90} of withanolide **10** (E,F), withanolide **12** (G,H) and withanolide **7** (I,J) during 24 h. Negative control of the parasite without any treatment (A,B) and the positive control with IC_{90} of miltefosine (C,D). Autophagic vacuoles with blue fluorescence are indicated with an arrow. The 100X images were captured using an EVOS® FL Cell Imaging System. Scale-bar: 20 µm.

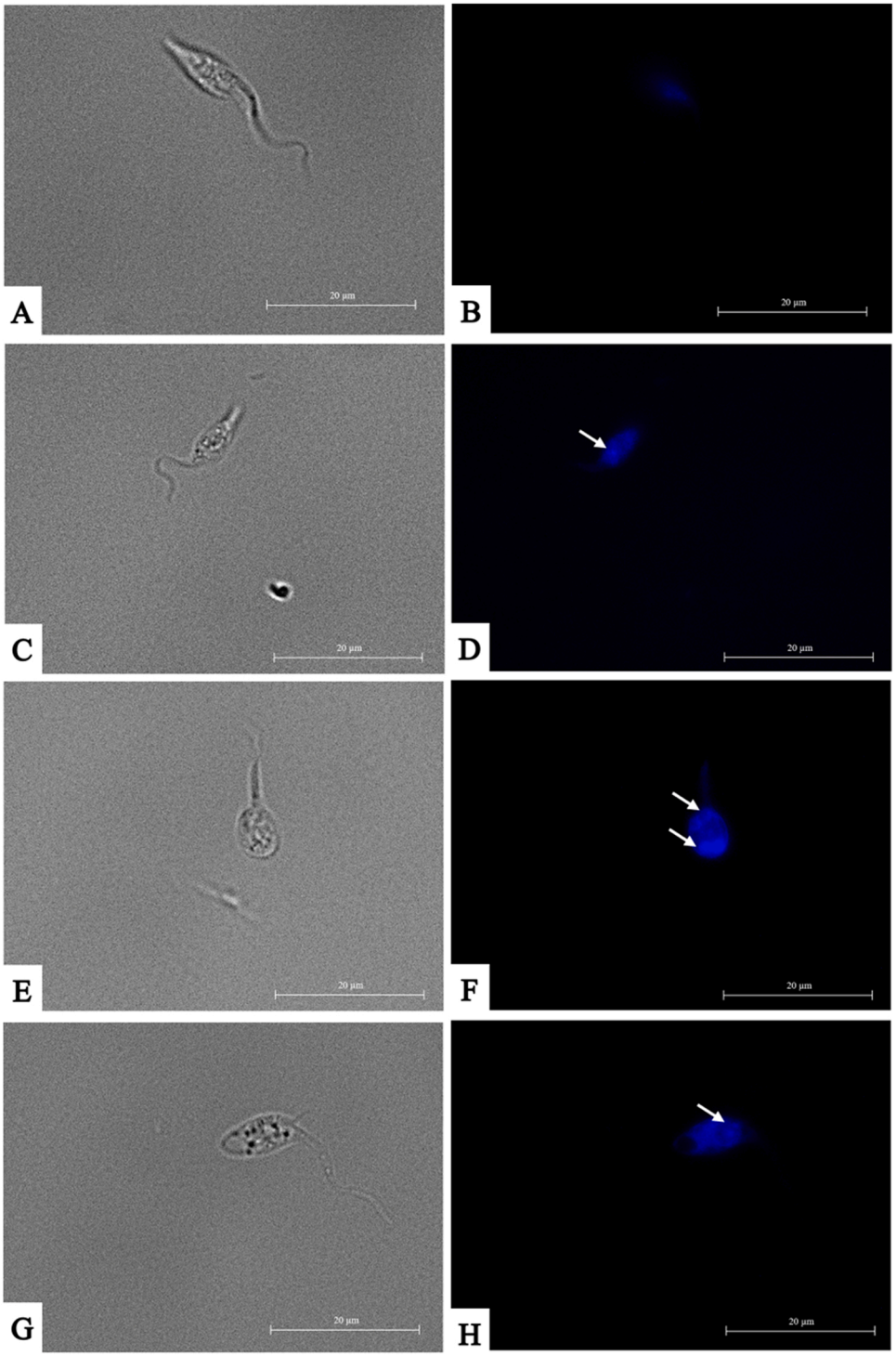

Fig. 10. *T. cruzi* epimastigotes incubated with IC_{90} of withanolide **10** (E,F) and withanolide **12** (G,H) during 24 h. Negative control of the parasite without any treatment (A,B) and the positive control with IC_{90} of benznidazole (C,D). Autophagic vacuoles with blue fluorescence are indicated with an arrow. The 100X images were captured using an EVOS® FL Cell Imaging System. Scale-bar: 20 µm.

demonstrated the high potential of withaferin A analogs to induce cell death by apoptosis in cancer cells. Moreover, this PCD had been evidenced by detection of DNA fragmentation, chromatin condensation and exposure of phosphatidylserine residues in cancer cells [38,39]. In addition, recent studies have shown that WA causes apoptosis-like cell death in *Leishmania donovani* by inhibiting protein kinase C (an important element in the apoptosis signaling pathways). Inhibition of this important enzyme causes depolarization of the mitochondrial membrane potential, generates reactive oxygen species (ROS) inside the parasites and DNA fragmentation occurs [40,41]. The results of the present study are in agreement with these previous studies, as a decrease in ATP levels, chromatin condensation and the presence of reactive oxygen species were detected in promastigotes and epimastigotes of *L. amazonensis* and *T. cruzi* treated with the selected withanolides (withanolides **7**, **10** and **12**). Moreover, in the case of *T. cruzi* epimastigotes there is a significant alteration of the mitochondrial

membrane potential. Furthermore, these compounds generated autophagic vacuoles in both parasites, which may also be an indication that autophagic processes are taking place. These results are consistent with previous research linking apoptosis and autophagy. These studies show that different drugs induce early autophagy that later evolves into similar cell death by apoptosis. In a recent review by Das P. et al. [42], different examples are reported, such as the case of cryptolepine, which generates autophagic vacuoles in *L. donovani* (positive for MCD) and from them different events characteristic of apoptosis such as DNA fragmentation occur. According to these results, it has been proposed that at low doses of some drugs autophagy can be initially activated as a survival mechanism in trypanosomatids, but if these conditions of cellular stress persist, the parasites would activate their cell death pathway by apoptosis-like. Based on all this evidence, withanolides **7**, **10** and **12** could induce early autophagy, which could evolve into apoptosis-like in both parasites, making them important candidates for future drugs against leishmaniasis and Chagas disease.

4. Conclusions

WA-derived silicon ethers showed promising activity against promastigotes and amastigotes of *L. amazonensis*, as well as against epimastigotes of *T. cruzi*. However, *L. donovani* promastigotes appear to be resistant to these withanolides. Among the 24 synthetic withanolides tested, three of them corresponding to withanolides **7**, **10** and **12** (27-Dimethyl WA, 27-Terbutyldimethyl WA and 4,27-Dimethylphenyl WA) stood out for their good leishmanicidal and trypanocidal activity, being almost twice as selective as the reference drugs miltefosine and benznidazole. Furthermore, the results obtained show that these three withanolides induce some changes in the parasites such as alteration of ATP levels, mitochondrial membrane potential, chromatin condensation, formation of reactive oxygen species and autophagic vacuoles in both *L. amazonensis* promastigotes and *T. cruzi* epimastigotes. These results demonstrate that the tested withanolides induce a programmed cell death event in the parasites and therefore, could be considered as promising candidates as future drugs against leishmaniasis and Chagas disease.

Funding

This work was funded by Instituto de Salud Carlos III, FIS (Ministerio Español de Salud, Madrid, Spain) FEDER, Spain [Project PI18/01380], Consorcio Centro De Investigacion Biomédica En Red (CIBER) de Enfermedades Infecciosas (CIBERINFEC) , Inst. de Salud Carlos III, Madrid, Spain [CB21/13/00100] and RICET Project [RD16/0027/0001] from Programa Redes Temáticas de Investigación Cooperativa. This work was also supported by Spanish Ministry of Economy and Competitiveness (MINECO), cofounded by the European Regional Development Fund (FEDER) grant [RTI2018-094356-B-C21]. D.S.N.-H. (TESIS2019010065) and C.J.B.-E. (TESIS2020010057) was funded by a grant from the Agencia Canaria de Investigación, Innovación y Sociedad de la Información cofunded by FEDER.

CRediT authorship contribution statement

D.S.N.-H., C.J.B.-E., A.L.-A., I.S.: Methodology. **E.H.A., I.A.J., I.L.B.**: Synthesis chemical compounds. **D.S.N.-H., C.J.B.-E., A.L.-A., I.S.**: Software. **J.E.P., J.L.M., I.A.J.**: Validation. **J.E.P., J.L.M.**: Formal analysis. **D.S.N.-H., C.J.B.-E., A.L.-A., I.S.**: Investigation. **J.E.P., J.L.M., I.A.J.**: Resources. **D.S.N.-H., C.J.B.-E., A.L.-A., I.S.**: Data curation. **D.S.N.-H., A.L.-A.**: Writing – original draft. **J.E.P., J.L.M., I.A.J.**: Writing – review & editing. **J.E.P., J.L.M., I.A.J.**: Visualization. **J.E.P., J.L.M.**: Supervision. **J.E.P., J.L.M.**: Project administration. **J.E.P., J.L.M.**: Funding acquisition. All authors have read and agreed to the published version of the manuscript.

Ethics approval

Not applicable.

Informed Consent Statement

Not applicable.

Data in brief

Supplementary material data is attached to the file. S1: Plasmatic membrane permeability assay. S2: Chromatin condensation analysis. S3: Analysis of reactive oxygen species.

Data availability

Data is contained within the article and the supplementary material.

Conflict of interest statement

The authors declare that they have no known competing financial interests or personal relationships that could have appeared to influence the work reported in this paper.

Acknowledgements

This study was supported by the RICET (project no. RD16/0027/0001 of the programme of Redes Temáticas de Investigación Cooperativa, FIS), CIBER de Enfermedades Infecciosas, Instituto de Salud Carlos III (CB21/13/00100), Spanish Ministry of Science, Innovation and Universities (MICINN), State Research Agency (AEI), the European Regional Development Funds (ERDF) (PGC2018-094503-B-C21), Ministerio de Sanidad, Gobierno de España and by the project N°: 21/0587 funded by the 'Cabildo de Tenerife, Tenerife Innova, MEDI and FDCAN. D.S.N.-H. was funded by a grant from Agencia Canaria de Investigación, Innovación y Sociedad de la Información (ACIISI) cofunded by Fondo Social Europeo (FSE) y FEDER, (TESIS2019010065). This work was also possible thanks to Spanish Ministry of Economy and Competitiveness (MINECO), cofounded by the European Regional Development Fund (FEDER) grant (RTI2018-094356-B-C21). Thanks La Laguna University and Ministry of Science and Innovation for a Junior Postdoctoral contract.

Appendix A. Supporting information

Supplementary data associated with this article can be found in the online version at doi:10.1016/j.biopha.2022.114012.

References

[1] Neglected tropical diseases. In: World Health Organization, 2022. ⟨http://www.emro.who.int/health-topics/tropical-diseases/⟩ Accessed 03 Feb 2022.
[2] Leishmaniasis. In: World Health Organization, 2022. ⟨https://www.who.int/news-room/fact-sheets/detail/leishmaniasis⟩ Accessed 03 Feb 2022.
[3] Chagas disease (American trypanosomiasis). In: World Health Organization, 2022. ⟨https://www.who.int/health-topics/chagas-disease#tab=tab_1⟩ Accessed 03 Feb 2022.
[4] L.A. González, S. Robledo, Y. Upegui, G. Escobar, W. Quiñones, Synthesis and evaluation of trypanocidal activity of chromane-type compounds and acetophenones, Molecules (2021). https://doi.org/10.3390/molecules26237067.
[5] Parasites-Leishmaniasis-Biology. In: Centers for Disease Control and Prevention, 2020. ⟨https://www.cdc.gov/parasites/leishmaniasis/biology.html⟩ Accessed 03 Feb 2022.
[6] Leishmaniasis-Epidemiology & Risk Factors. In: Centers for Disease Control and Prevention, 2020. ⟨https://www.cdc.gov/parasites/leishmaniasis/epi.html⟩ Accessed 03 Feb 2022.
[7] Parasites- American Trypanosomiasis (also known as Chagas disease)- Detailed FAQs. In: Centers for Disease Control and Prevention, 2022. ⟨https://www.cdc.gov/parasites/chagas/gen_info/detailed.html⟩ Accessed 03 Feb 2022.

[8] Parasites- American Trypanosomiasis (also known as Chagas disease)- Disease. In: Centers for Disease Control and Prevention, 2019. ⟨https://www.cdc.gov/parasites/chagas/disease.html⟩ Accessed 03 Feb 2022.

[9] L.S. Sangenito, V. da Silva Santos, C.M. d'Avila-Levy, M.H. Branquinha, A.L. Souza Dos Santos, S. de Oliveira, Leishmaniasis and Chagas disease - neglected tropical diseases: treatment updates, Curr. Top. Med. Chem. (2019), https://doi.org/10.2174/1568026619031903281551 36.

[10] A. López-Arencibia, D. San Nicolás-Hernández, C.J. Bethencourt-Estrella, I. Sifaoui, M. Reyes-Batlle, R.L. Rodríguez-Expósito, A. Rizo-Liendo, J. Lorenzo-Morales, I. L. Bazzocchi, J.E. Piñero, I.A. Jiménez, Withanolides from *Withania aristata* as antikinetoplastid agents through induction of programmed cell death, Pathogens (2019), https://doi.org/10.3390/pathogens8040172.

[11] S.J. Cruz, Más de 100 Plantas Medicinales. Medicina Popular Canaria Monografías. In Pérez Galdós editors. Obra Social de La Caja de Canarias. Las Palmas de Gran Canaria, España, 2007.

[12] N.R. Perestelo, G.G. Llanos, C.P. Reyes, A. Amesty, K. Sooda, S. Afshinjavid, I. A. Jiménez, F. Javid, I.L. Bazzocchi, Expanding the chemical space of Withaferin A by incorporating silicon to improve its clinical potential on human ovarian carcinoma cells, J. Med. Chem. (2019), https://doi.org/10.1021/acs.jmedchem.9b00146.

[13] X. Zhang, A.K. Samadi, K.F. Roby, B. Timmermann, M.S. Cohen, Inhibition of cell growth and induction of apoptosis in ovarian carcinoma cell lines CaOV3 and SKOV3 by natural withanolide Withaferin A, Gynecol. Oncol. (2012), https://doi.org/10.1016/j.ygyno.2011.11.044.

[14] A.K. Franz, S.O. Wilson, Organosilicon molecules with medicinal applications, J. Med. Chem. 56 (2) (2013) 388–405, https://doi.org/10.1021/jm3010114.

[15] W.R. Proto, G.H. Coombs, J.C. Mottram, Cell death in parasitic protozoa: regulated or incidental, Nat. Rev. Microbiol. 11 (1) (2013) 58–66, https://doi.org/10.1038/nrmicro2929.

[16] J.V. Silva-Silva, C.J. Moragas-Tellis, M. Chagas, P. Souza, D.L. Moreira, D. J. Hardoim, N.N. Taniwaki, V. Costa, A.L. Bertho, D. Brondani, E. Zapp, A.S. de Oliveira, K.S. Calabrese, M.D. Behrens, F. Almeida-Souza, Carajurin induces apoptosis in Leishmania amazonensis promastigotes through reactive oxygen species production and mitochondrial dysfunction, Pharmaceuticals 15 (3) (2022) 331, https://doi.org/10.3390/ph15030331.

[17] O. Chiboub, I. Sifaoui, M. Abderrabba, M. Mejri, J.J. Fernández, A.R. Díaz-Marrero, J. Lorenzo-Morales, J.E. Piñero, Apoptosis-like cell death upon kinetoplastid induction by compounds isolated from the brown algae Dictyota spiralis, Parasites Vectors 14 (1) (2021) 198, https://doi.org/10.1186/s13071-021-04693-7.

[18] W. de Souza, M. Attias, J.C. Rodrigues, Particularities of mitochondrial structure in parasitic protists (Apicomplexa and Kinetoplastida, Int. J. Biochem. Cell Biol. (2009), https://doi.org/10.1016/j.biocel.2009.04.007.

[19] L. Basmaciyan, M. Casanova, Cell death in Leishmania. La mort cellulaire chez Leishmania, Parasite (2019), https://doi.org/10.1051/parasite/2019071.

[20] R. Menna-Barreto, Cell death pathways in pathogenic trypanosomatids: lessons of (over)kill, Cell Death Dis. (2019), https://doi.org/10.1038/s41419-019-1370-2.

[21] M.J. Núñez, M.L. Martínez, A. López-Arencibia, C.J. Bethencourt-Estrella, D. San Nicolás-Hernández, I.A. Jiménez, J. Lorenzo-Morales, J.E. Piñero, I.L. Bazzocchi, *In Vitro* susceptibility of kinetoplastids to celastroloids from Maytenus chiapensis, Antimicrob. Agents Chemother. (2021), https://doi.org/10.1128/AAC.02236-20.

[22] C.J. Bethencourt-Estrella, N. Nocchi, A. López-Arencibia, D. San Nicolás-Hernández, M.L. Souto, B. Suárez-Gómez, A.R. Díaz-Marrero, J.J. Fernández, J. Lorenzo-Morales, J.E. Piñero, Antikinetoplastid activity of sesquiterpenes isolated from the Zoanthid *Palythoa aff. clavata*, Pharmaceuticals (2021), https://doi.org/10.3390/ph14111095.

[23] A. López-Arencibia, C. Martín-Navarro, I. Sifaoui, M. Reyes-Batlle, C. Wagner, J. Lorenzo-Morales, S.K. Maciver, J.E. Piñero, Perifosine mechanisms of action in Leishmania species, Antimicrob. Agents Chemother. (2017), https://doi.org/10.1128/AAC.02127-16.

[24] L. Cartuche, I. Sifaoui, A. López-Arencibia, C.J. Bethencourt-Estrella, D. San Nicolás-Hernández, J. Lorenzo-Morales, J.E. Piñero, A.R. Díaz-Marrero, J. J. Fernández, Antikinetoplastid activity of indolocarbazoles from *Streptomyces sanyensis*, Biomolecules (2020), https://doi.org/10.3390/biom10040657.

[25] C.J. Bethencourt-Estrella, S. Delgado-Hernández, A. López-Arencibia, D. San Nicolás-Hernández, I. Sifaoui, D. Tejedor, F. García-Tellado, J. Lorenzo-Morales, J. E. Piñero, Acrylonitrile derivatives against *Trypanosoma cruzi*: in vitro activity and programmed cell death study, Pharmaceuticals (2021), https://doi.org/10.3390/ph14060552.

[26] A.R. Díaz-Marrero, A. López-Arencibia, C.J. Bethencout-Estrella, F. Cen-Pacheco, I. Sifaoui, A. Hernández Creus, M.C. Duque-Ramírez, M.L. Souto, A. Hernández Daranas, J. Lorenzo-Morales, J.E. Piñero, J.J. Fernández, Antiprotozoal activities of marine polyether triterpenoids, Bioorg. Chem. (2019), https://doi.org/10.1016/j.bioorg.2019.103276.

[27] I. Sifaoui, I. Rodríguez-Talavera, M. Reyes-Batlle, R.L. Rodríguez-Expósito, P. Rocha-Cabrera, J.E. Piñero, J. Lorenzo-Morales, *In vitro* evaluation of commercial foam Belcils® on Acanthamoeba spp, Int. J. Parasitol. Drugs Drug Resist. (2020), https://doi.org/10.1016/j.ijpddr.2020.10.002.

[28] C.M. Adade, G.S. Chagas, T. Souto-Padrón, Apis mellifera venom induces different cell death pathways in Trypanosoma cruzi, Parasitology (2012), https://doi.org/10.1017/S0031182012000790.

[29] A. Singh, A. Raza, S. Amin, C. Damodaran, A.K. Sharma, Recent advances in the chemistry and therapeutic evaluation of naturally occurring and synthetic withanolides, Molecules (2022), https://doi.org/10.3390/molecules27030886.

[30] R. Lin, Y.Z. Guan, R.J. Li, X.M. Xu, J.G. Luo, L.Y. Kong, 13,14-seco-Withanolides from Physalis minima with potential anti-inflammatory activity, Chem. Biodivers. 13 (7) (2016) 884–890, https://doi.org/10.1002/cbdv.201500282.

[31] F. Gutiérrez Nicolás, G. Reyes, M.C. Audisio, M.L. Uriburu, S. Leiva González, G. E. Barboza, V.E. Nicotra, Withanolides with antibacterial activity from Nicandra john-tyleriana, J. Nat. Prod. 78 (2) (2015) 250–257, https://doi.org/10.1021/np500824f.

[32] G. Xia, Y. Li, J. Sun, L. Wang, X. Tang, B. Lin, N. Kang, J. Huang, L. Chen, F. Qiu, Withanolides from the stems and leaves of Physalis pubescens and their cytotoxic activity, Steroids 115 (2016) 136–146, https://doi.org/10.1016/j.steroids.2016.09.002.

[33] M. Kuroyanagi, M. Murata, T. Nakane, O. Shirota, S. Sekita, H. Fuchino, Z. K. Shinwari, Leishmanicidal active withanolides from a pakistani medicinal plant, Withania coagulans, Chem. Pharm. Bull. 60 (7) (2012) 892–897, https://doi.org/10.1248/cpb.c12-00264.

[34] M.I. Choudhary, S. Yousaf, S. Ahmed, Samreen, K. Yasmeen, Atta-ur-Rahman, Antileishmanial physalins from Physalis minima, Chem. Biodivers. 2 (9) (2005) 1164–1173, https://doi.org/10.1002/cbdv.200590086.

[35] S. Nagafuji, H. Okabe, H. Akahane, F. Abe, Trypanocidal constituents in plants 4. Withanolides from the aerial parts of Physalis angulata, Biol. Pharm. Bull. (2004), https://doi.org/10.1248/bpb.27.193.

[36] M. Suffness, J.M. Pezzuto, Assays related to cancer drug discovery, in: K. Hostettmann (Ed.), Methods in Plant Biochemistry: Assays for Bioactivity, Academic Press, London, 1991, pp. 71–133.

[37] S. Lima, J. Pacheco, A.M. Marques, E. Veltri, R.C. Almeida-Lafetá, M.R. Figueiredo, M. Kaplan, E.C. Torres-Santos, Leishmanicidal activity of Withanolides from *Aureliana Fasciculata* var. *Fasciculata*, Molecules (2018), https://doi.org/10.3390/molecules23123160.

[38] G.G. Llanos, L.M. Araujo, I.A. Jiménez, L.M. Moujir, J. Rodríguez, C. Jiménez, I. L. Bazzocchi, Structure-based design, synthesis, and biological evaluation of withaferin A-analogues as potent apoptotic inducers, Eur. J. Med. Chem. (2017), https://doi.org/10.1016/j.ejmech.2017.09.004.

[39] L. Li, B. Niu, W. Zhang, L. Hou, Y. Zheng, Withaferin A inhibits cell proliferation of U266B1 and IM-9 human myeloma cells by inducing intrinsic apoptosis, Acta Biochim. Pol. (2022), https://doi.org/10.18388/abp.2020_5938.

[40] N. Sen, B. Banerjee, B.B. Das, A. Ganguly, T. Sen, S. Pramanik, S. Mukhopadhyay, H.K. Majumder, Apoptosis is induced in leishmanial cells by a novel protein kinase inhibitor withaferin A and is facilitated by apoptotic topoisomerase I-DNA complex, Cell Death Differ. (2007), https://doi.org/10.1038/sj.cdd.4402002.

[41] A. Grover, S.P. Katiyar, J. Jeyakanthan, V.K. Dubey, D. Sundar, Blocking protein kinase C signaling pathway: mechanistic insights into the anti-leishmanial activity of prospective herbal drugs from Withania somnifera, BMC Genom. (2012), https://doi.org/10.1186/1471-2164-13-S7-S20.

[42] P. Das, S. Saha, S. BoseDasgupta, The ultimate fate determinants of drug induced cell-death mechanisms in Trypanosomatids, Int. J. Parasitol. Drugs Drug Resist. (2021), https://doi.org/10.1016/j.ijpddr.2021.01.003.